Polymer 51 (2010) 774–782

Contents lists available at ScienceDirect

Polymer

journal homepage: www.elsevier.com/locate/polymer

Hierarchical structure of injection-molded bars of HDPE/MWCNTs composites with novel nanohybrid shish–kebab

Jinghui Yang, Ke Wang, Hua Deng, Feng Chen, Qiang Fu*

Department of Polymer Science and Materials, State Key Laboratory of Polymer Materials Engineering, Sichuan University, Chengdu 610065, PR China

ARTICLE INFO

Article history:
Received 11 October 2009
Received in revised form
27 November 2009
Accepted 28 November 2009
Available online 3 December 2009

Keywords:
Nanohybrid shish–kebab
Hierarchical structure
Injection molding

ABSTRACT

Injection-molded products usually show hierarchical structure from skin to core due to the existence of shear gradient and temperature gradient. Investigating the hierarchical structure is helpful to better understand the structure-property relationship of injection-molded sample, which is important for design and preparation of polymer products with high performance. In this work, the hierarchical structures of injection-molded bars of high-density polyethylene (HDPE)/multi-walled carbon nanotubes (MWCNTs) composite were explored by examining the microstructure and crystal morphology, layer by layer, along the sample thickness, using SEM, DSC and 2D-WAXS. To enhance the shear effect, a so-called dynamic packing injection molding (DPIM) technique was used to prepare the molded bar with high orientation level. Interestingly, SEM revealed that in the skin and core zones, the lamellae of PE anchored randomly on the surface of MWCNTs, while well-defined nanohybrid shish–kebab (NHSK) entities, in which fibrillous carbon nanotubes (CNTs) act as shish while HDPE lamellae act as kebab, exist in the oriented zone. The changed NHSK crystal structure along the thickness direction of molded bar is considered as due to the shear gradient and thermal gradient in injection molding. And the underlying origin of in situ formation of NHSK under shear effects is discussed based on experimental observations.
© 2009 Elsevier Ltd. All rights reserved.

1. Introduction

Due to their extraordinary mechanical, electrical, and optical properties, carbon nanotubes (CNTs) have attracted tremendous attentions in recent years [1–3]. Polymer/CNT nanocomposite (PCN) is one of the most promising fields for the application of CNTs, which oftentimes exhibits excellent properties that differ substantially from those of pristine polymer matrix. Good dispersion and strong interfacial adhesions are the two issues to ensure success of fabricating polymer/CNTs composites with excellent properties [4]. Therefore, in general, functionalizing or modifying of CNTs is necessary before compounding with polymers. Various strategies, such as grafting modification [5–7], special processing methods [8,9], have been reported, although these strategies are complicated and of low production efficiency.

It is well-known that shish–kebab structure is formed via shear or elongational flow fields in melts or solution [10–14], which consists of stretched polymer chains as shish surrounded by folded-chain lamellae as kebab periodically attached along the shish. Recently, a novel nanohybrid shish–kebab (NHSK) superstructure has been observed in polymer/CNTs composites, in which fibrillous carbon nanotubes (CNTs) act as shish while high-density polyethylene (HDPE) lamellae act as kebab, which has been regarded as a new strategy of functionalizing of CNTs to alter the surface properties of CNTs and enhance the interfacial interaction between polymers and CNTs [15]. This novel superstructure was first reported by Li et al. [16]. They have successfully grown polyethylene and Nylon 6, 6 on carbon nanotubes via solution crystallization; meanwhile the "size-dependent soft epitaxy" was proposed to explain the NHSK formation mechanism [17]. Even more, the fine structure of NHSK could be further controlled via aid of supercritical CO_2 [18–20].

By far, the most-reported method to obtain NHSK superstructure of polymer/CNTs involves a strict procedure of solution crystallization. In our previous work, the fine nanohybrid shish–kebab superstructure was first achieved directly in the injection-molded bar of HDPE/whiskers and HDPE/CNTs composite [21,22], using a so-called dynamic packing injection molding technology (DPIM), in which oscillatory shear field was imposed on the gradually cooled melt during the packing solidification stage. Such in situ formation of NHSK structure in the injection molding process is attributed to the external shearing effect and subsequently soft epitaxy of polymer crystallization on CNTs. Meanwhile, the greatly improved enhancement of mechanical properties has been

* Corresponding author. Tel.: +86 28 85405402.
E-mail address: qiangfu@scu.edu.cn (Q. Fu).

0032-3861/$ – see front matter © 2009 Elsevier Ltd. All rights reserved.
doi:10.1016/j.polymer.2009.11.059

achieved via the formation of NHSK structure. Since injection-molded products usually show hierarchical structure from the skin to the core due to the existence of shear gradient and temperature gradient, a more complicated hierarchical structure is expected in such dynamic packing injection-molded bar, comparing with that in the conventional injection-molded bar. Thus the purpose of this work is to investigate the hierarchical structures of the injection-molded bars of HDPE/MWCNTs composites, layer by layer, along the sample thickness, using SEM, DSC and 2D-WAXS, to further understand formation mechanism of NHSK structures in the injection molding process. It is due to the shear gradient and thermal gradient in injection molding that a hierarchical structure with changed NHSK crystal structure along the thickness direction of molded bar can be directly observed by SEM. And the underlying origin of in situ formation of NHSK under shear effect is discussed based on the results of DSC.

2. Experimental section

2.1. Materials and preparation of composite

HDPE with a trade name 2911, was used as the matrix. It had a melt flow index of 20 g/10 min and molecular weight (M_w) of 1.2×10^5, and it was supplied by Fushun Petrochemical Corp. Raw MWCNTs were purchased from Shenzhen Nanotechnology Co. Ltd. The main range of diameter of the raw MWCNTs was about 10–20 nm and their length was about 5–15 μm, the purity was lager than 95%, and ash (catalyst residue) is less than 0.2%. MWCNTs were used without any pretreatment. The content of MWCNTs is 3%. After being dried in 70 °C for 12 h in a vacuum environment, MWCNTs were blended with HDPE using a corotating twinscrew extruder (TSSJ-25) with a barrel temperature of 150 °C. After being pelletized and dried, the blends were injected into a mold with aid of an SZ 100 g injection molding machine with a barrel temperature of 180 °C and injection pressure of 90 MPa. In order to prepare materials containing highly oriented structure, special molded equipment named as dynamic packing injection molding (DPIM) was attached on the injection machine. The processing parameters and the characteristics and detail experiment procedure of DPIM were described elsewhere. [23,24] The main feature of DPIM is that the melt is first injected into the mold then forced to move repeatedly in a chamber by two pistons that moved reversibly with the same frequency as the solidification progressively occurs from the mold wall to the molding core part. We also prepared the "static" specimens by using the conventional molding technology for comparison purpose. Generally speaking, for a conventional injection-molded bar, which subjects to relaxation and solidification under quiescent conditions, along its thickness direction there exist skin and core layers. On the other hand, the relaxation of oriented chains can be suppressed and fixed during melt solidification via DPIM, resulting in a high orientation of molecular chains and anisotropic morphology, with the main feature of the shear-induced morphologies with core in the center, oriented zone surrounding the core and the skin layer in the cross-sectional areas of the samples, as shown in Fig. 1.

2.2. Characterizations

2.2.1. Scanning electron microscopy (SEM)

The evaluation of microstructure and crystal morphology in injected-molding bar becomes much complicated because the existence of a shear gradient and a temperature gradient from the skin to the core of the samples. So a skin-core morphology with changed orientation and lamellae size along the thickness direction of molded bar is expected. To check the lamellae structure, the specimen obtained with a thickness of 3.4 mm (3400 μm), was cryogenically fractured in the direction parallel to flow direction in liquid nitrogen, and etched by 1% solution of potassium permanganate in a mixture of sulphuric acid, 85% orthophosphoric acid and water [24]. Then the etched surface was coated with gold and examined from the skin to the core, layer by layer along the thickness direction as shown in Fig. 2, by a SEM instrument (Inspect F, FEI Company) operation at 20 kV.

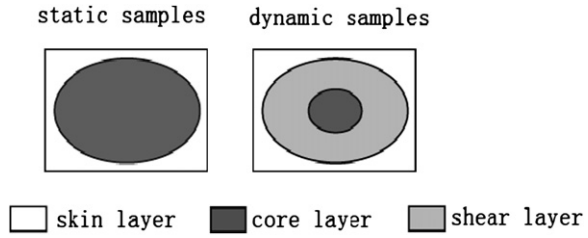

Fig. 1. Macroscopic features of injection-molded samples obtained: (a) static samples; (b) dynamic samples.

2.2.2. Differential scanning calorimetry (DSC)

A Perkin–Elmer diamond-II differential scanning calorimetric (DSC) was used to determine the melting behavior of the injection-molded specimen. For a layer by layer exanimation of melting behavior, the slices were cut from the near surface to the core along the sample thickness, indicated as the same as Fig. 2. Then the cut slices were heated from 20 to 170 °C at a heating rate of 10 °C/min under a nitrogen atmosphere.

2.2.3. Synchrotron two-dimensional wide-angle X-ray scattering (2D-WAXS)

Synchrotron WAXD experiments were carried out at room temperature upon the U7B beam line in the National Synchrotron Radiation Laboratory (NSRL), University of Science and Technology of China, Hefei. The wavelength used is 0.1409 nm. The two-dimensional (2D) WAXD patterns were recorded in every 180 s by a Mar CCD 165 X-ray detector system. The Fit2D software package was used to analyze the 2D WAXD patterns. Azimuthal scans (0–360°) of WAXS were made for the (110) plane of HDPE. The orientation level of various planes could be calculated by the orientation parameter f,

$$f = \frac{3\langle \cos^2 \varphi \rangle - 1}{2} \quad (1)$$

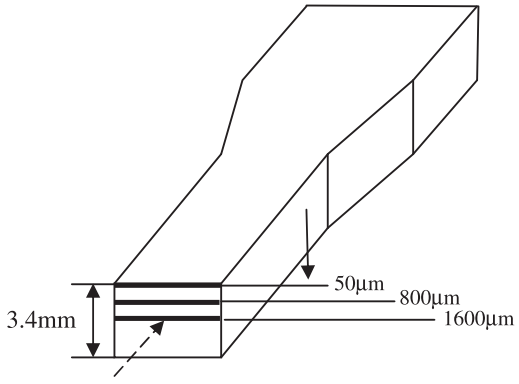

Fig. 2. Schematic diagram of specimen preparation for structure characterization.

$$\left\langle \cos^2\varphi \right\rangle = \frac{\int_0^{\frac{\pi}{2}} I(\phi)\sin\phi\cos\phi\,\mathrm{d}\phi}{\int_0^{\frac{\pi}{2}} I(\phi)\sin\phi\,\mathrm{d}\phi} \quad (2)$$

where φ is the angle between the normal of a given (hk0) crystal plane and the shear flow direction and I is the intensity. The critical values of orientation parameter f, taking $\varphi = 0$ as the shear flow direction, are -0.5 for a perfect perpendicular orientation and 1.0 for a perfect parallel orientation. For an isotropic sample, $f = 0$.

3. Results and discussion

3.1. Orientation of injection-molded bar of HDPE/MWCNTs composites

2D-WAXS was used to investigate orientation of HDPE/MWCNTs composites. 2D-WAXS patterns of static and dynamic samples of HDPE/MWCNTs composites containing 3 wt% of MWCNTs are shown in Fig. 3, where the diffraction signals are designated to the (110) plane and (200) plane of orthorhombic PE lamellae, and the number represents the distance away from the sample surface. For static samples, two strong diffraction focused arcs are found in the skin layer (50 μm), while the isotropic circles are observed for the intermediate and core layers (800 μm and 1600 μm) as shown in Fig. 3(a), indicating a random orientation via conventional injection molding. Fig. 3(b) shows the 2D-WAXS patterns of dynamic samples of HDPE/MWCNTs composites. One observes strong reflections of (110) and (200) planes at the meridian, indicating a preferential orientation along shear direction. However, the oriented structure exists only in the skin and shear layer even for dynamic samples. In the core layer, the isotropic circles are observed in Fig. 3(b) (1600 μm), indicating a random molecular orientation. The orientation degrees of various layers of static samples and dynamic samples are calculated and listed in Table 1. The orientation degrees of static samples for various layers are 0.69, 0.17, 0.19 from skin to core, and 0.71, 0.86, 0.87, 0.19 for dynamic samples. It is clear that comparing with static samples, the orientation of dynamic samples is strengthened by the shear exposed by DPIM, showing the high orientation degree in the oriented layer. This result is well coordinated with the pure polymer [25] and polymer/filler composites [26] obtained via DPIM.

3.2. Hierarchical structure with novel nanohybrid shish–kebab structure

SEM examination of the etched surface cut from the section parallel to flow direction provides important morphological information of static and dynamic samples. Fig. 4 shows the crystalline morphology of various layers of static samples (Fig. 4(a)) and dynamic samples (Fig. 4(b)) of pure HDPE, from skin to core layers. One can observe the oriented lamellae structure in the skin at 50 μm away from the surface and spherulite-like structure at 800 μm and 1600 μm, respectively. The oriented lamellae structure in skin layer is derived from the fast cooling and freezing of polymer chains, while the increased relaxation of polymer chains cause a random arranged lamellae in the core. For the dynamic samples of pure HDPE, shear field is imposed on the melts during packing processing, resulting in strengthened orientation of composites. The formation of oriented layer between the skin region and core region yields complicated structural hierarchy in the injection-molded bar. The evolution of crystalline morphology is clearly seen along the sample thickness. At the skin (50 μm), one observes the loose lamellae assembly perpendicular to the flow direction, and there also exist some twisted growths of lamellae. Ordered arranged lamellae along the flow directions are found when the distance is 800 μm from the surface (in the oriented layer). In the core at the distance of 1600 μm, the cluster-like crystalline with randomly distributed lamellae are clearly observed. These results are consistent well with that of 2D-WAXS and other literatures [27,28], representing the typical hierarchical structure of HDPE obtained by DPIM.

On the other hand, for the HDPE/MWCNTs composite, the crystalline morphologies of injection-molded bar are shown in Fig. 5 and Fig. 6 for static and dynamic sample, respectively. For static sample, the crystalline morphology induced by MWCNTs in skin and core region shows somewhat disparity, as shown in Fig. 5. A few lamellae are randomly distributed on the MWCNTs. The phenomenon is ascribed to the preferential heterogeneous nucleation at the interface of MWCNTs. In the core layer, some lamellae randomly disperse on the surface of MWCNTs. Obviously, the fast cooling in skin layer leads to a partial orientation of lamellae, while increased relaxation of polymer chain causes the spherulite-like structure in the core layer. The hierarchical structures of dynamic sample along the thickness direction are shown in Fig. 6. The content of MWCNTs in this samples is 3 wt% as the same as the static sample. In the skin layer (the depth is 50 μm), the lamellae are loosely arranged along the flow direction as the same as the static samples of HDPE/MWCNTs composites shown in Fig. 5(a). For the shear layers, when the depth of samples increases to 400, 800, 1200 μm, due to the effect of shear, there exist dense packing of PE lamellae along the flow direction. It is interesting that the MWCNTs are decorated with disk-shaped lamellae that are periodically located along the MWCNTs, as shown in Fig. 6(b)–(d). These decorations are edge-on PE lamellae with an average lateral dimension of 50–100 nm. The periodicity of these wrapped PE lamellae varies from 40 to 80 nm. These are the main features of nanohybrid shish–kebab, as the same as reported by Li et al. [16,17]. It is worthy to be noticed that the longitudinal direction (the long axis of MWCNTs) of NHSK is not always parallel to the shear flow direction, although most of MWCNTs are incline to be parallel to the flow direction. However, whatever the long axis of CNTs is perpendicular to or parallel to the shear flow direction, the lamellae of PE are always perpendicular to long axis of CNTs, indicating a strong epitaxy growth of PE on the surface of CNTs under effect of shear. A careful comparison about crystalline morphology between the composites and pure HDPE indicates that the length of kebab in NHSK is obviously shorter than that in pure HDPE and the periodicity of PE lamellae is much wider than that in pure HDPE. More away from the surface of samples, at the near center of the sample (the depth is 1200–1600 μm), as shown in Fig. 6(e), a sudden change of crystalline morphology from dense packing lamellae structure to a random distributed lamellae superstructure is observed. One can also find some NHSK entities as shown by the arrow, but with irregular shape of lamellae and disordered pattern on the surface of MWCNTs.

The change of crystal morphology from random distributed lamellae structure at the skin, to the nanohybrid shish–kebab at the shear layer, up to the irregular pattern of lamellae on the surface of MWCNTs in core region of the DPIM injection-molded bar will be discussed in a viewpoint of formation of NHSK. The change of crystal morphology is closely related to the temperature gradient and shear stress gradient along the thickness. The formation mechanism of NHSK was illustrated as the epitaxial growth of PE on MWCNT and geometric confinement, as suggested by Li et al. [16,17]. However, due to the effect of thermal history and shear in the injection molding, the

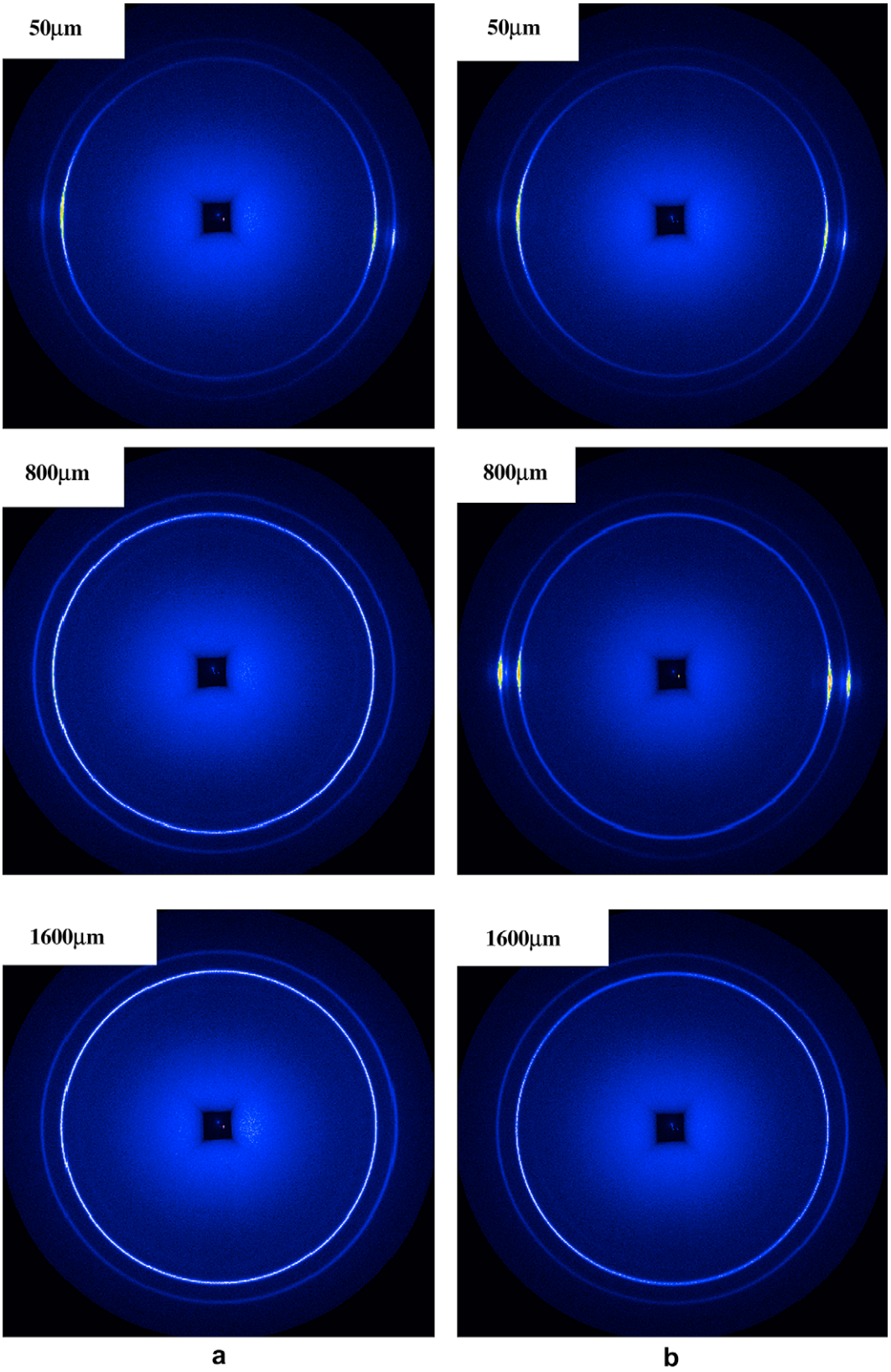

Fig. 3. 2D-WAXS patterns of various layers of HDPE/CNTs composites: (a)static samples; (b) dynamic samples.

formation mechanism of NHSK is somewhat different from that suggested by Li et al. Two nucleation paths [22] for MWCNTs in PE matrix to form the NHSK via DPIM are proposed: first, the MWCNTs with high nucleation efficiency can attract PE chains deposited on its surface and chain-fold occurs directly on the MWCNTs surface; the other is that the extended-chain PE shish is formed directly on the

Table 1
Oriented degrees of various layers of HDPE/CNTs composites obtained by 2D-WAXS for static samples and dynamic samples.

	Orientation degree		
	50 μm	800 μm	1600 μm
Dynamic samples	0.71	0.84	0.19
Static samples	0.69	0.17	0.19

MWCNTs surface before the formation of folded-chain lamellae. Therefore, variety of crystalline morphology from skin to core in injection-molded bar is assumed to be determined by the nucleation capability of MWCNTs and PE chain relaxation during processing. Obviously, the orientation of skin layer is derived from the fast cooling and corresponding shorter relaxation time of polymer chain. So the nucleation of MWCNTs is supposed to be weak. In the shear layer, when the shear is imposed on melts, coil chains are more incline to be

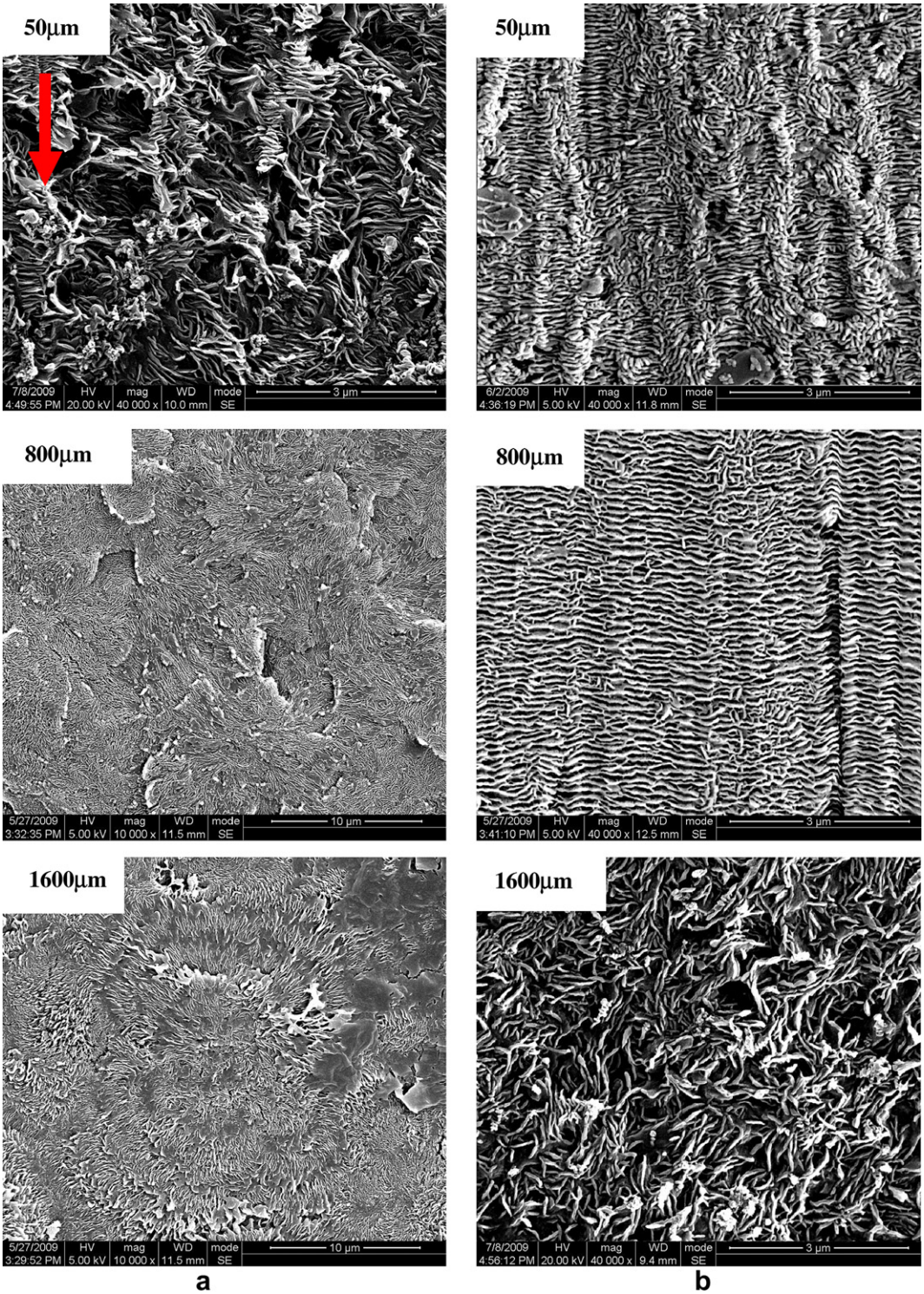

Fig. 4. SEM microphotographs of various layers of etched pure HDPE along the thickness direction: (a) static samples; (b) dynamic samples. The arrow shows the shear direction.

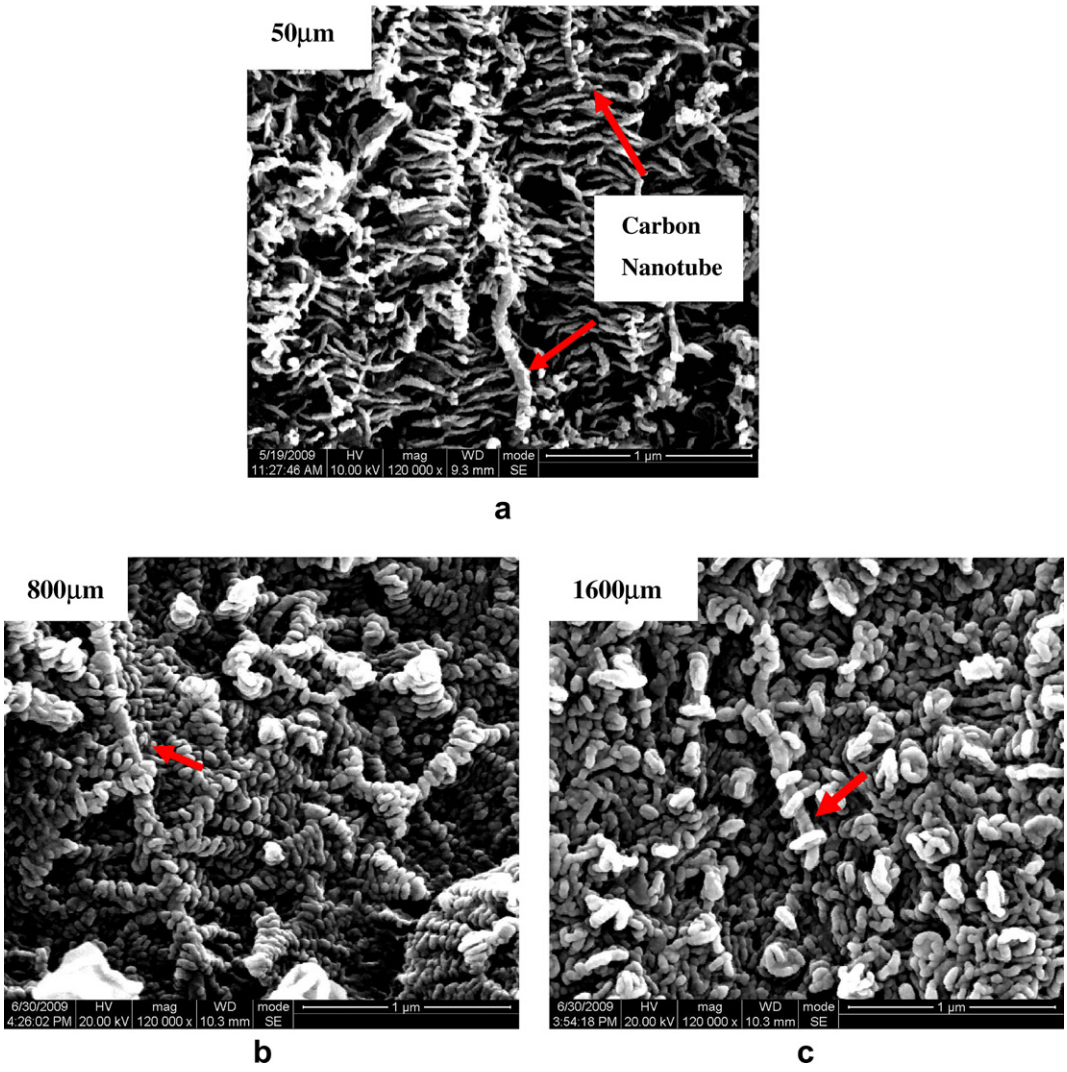

Fig. 5. SEM microphotographs of various layers of etched static HDPE/CNTs composites along the thickness direction: (a) 50 μm; (b) 800 μm; (d) 1600 μm.

stretched. The stretched chains have higher crystallization capability than the random, coiled chain due to the reduced crystallization barrier after being stretched. And also the stretched chains are inclined to attach on the surface of MWCNTs due to the geometric configuration of MWCNTs. After that the kebab grows perpendicular to the long axis of MWCNTs, obeying the "soft epitaxy" crystallization mechanism. Here the shear effect greatly improves the nucleation capability of MWCNTs, resulting in a great deal of lamellae decorated on the MWCNTs surface. Meanwhile the soft epitaxy concerning the geometric confinement arrangement helps the lamellae arrange themselves regularly. In the core region, a relatively higher temperature makes easy relaxation of polymer chains, thus resulting in randomly distributed lamellae. Thus, the nucleation effect of MWCNTs and chain relaxation of HDPE along the sample thickness are assumed to be the key points for the observed formation of crystalline morphologies, of course, and the main reasons for the hierarchical structure of injection-molded bars of HDPE/MWCNTs composites with novel nanohybrid shish–kebab structure.

3.3. DSC measurement

DSC is also an effective measurement to illustrate the crystalline structure. The changed crystal structure in the injection-molded samples along the thickness can be also demonstrated by DSC experiment. Fig. 7 shows the DSC heating curves at each layer of static samples for pure HDPE (Fig. 7(a)) and HDPE/MWCNTs composites (Fig. 7(b)). One can clearly observe only one peak at 130 °C for all layers except that the skin layer shows a shoulder peak at 133 °C. The shoulder peak may be related to the exothermic event of partially occurred re-crystallization melting, because in the skin zone the crystals are quite incomplete arisen from freezing the mobility of melt chains by fast cooling rate. It seems that MWCNTs make no difference for the melting of HDPE for the dynamic samples. DSC curves of various layers of dynamic samples, including the HDPE and HDPE/MWCNTs composites are shown in Fig. 8(a) and Fig. 8(b), respectively. One of the features of melting behavior of dynamic pure HDPE is that within the oriented region (400–1200 μm) the melting temperatures (around 133 °C) are significantly higher than that of skin (130 °C) and the widths of peaks are broadened. Oscillatory shear-induced crystallization into thicker lamellae is responsible for higher melting point in the oriented region, while the interplay of shear stress gradient and temperature gradient makes the crystallization process more complicated, which resulting in a broader distribution of crystal size and thus broadening the melting peaks. Again, for pure HDPE, an addition peak at a higher temperature is observed at the skin

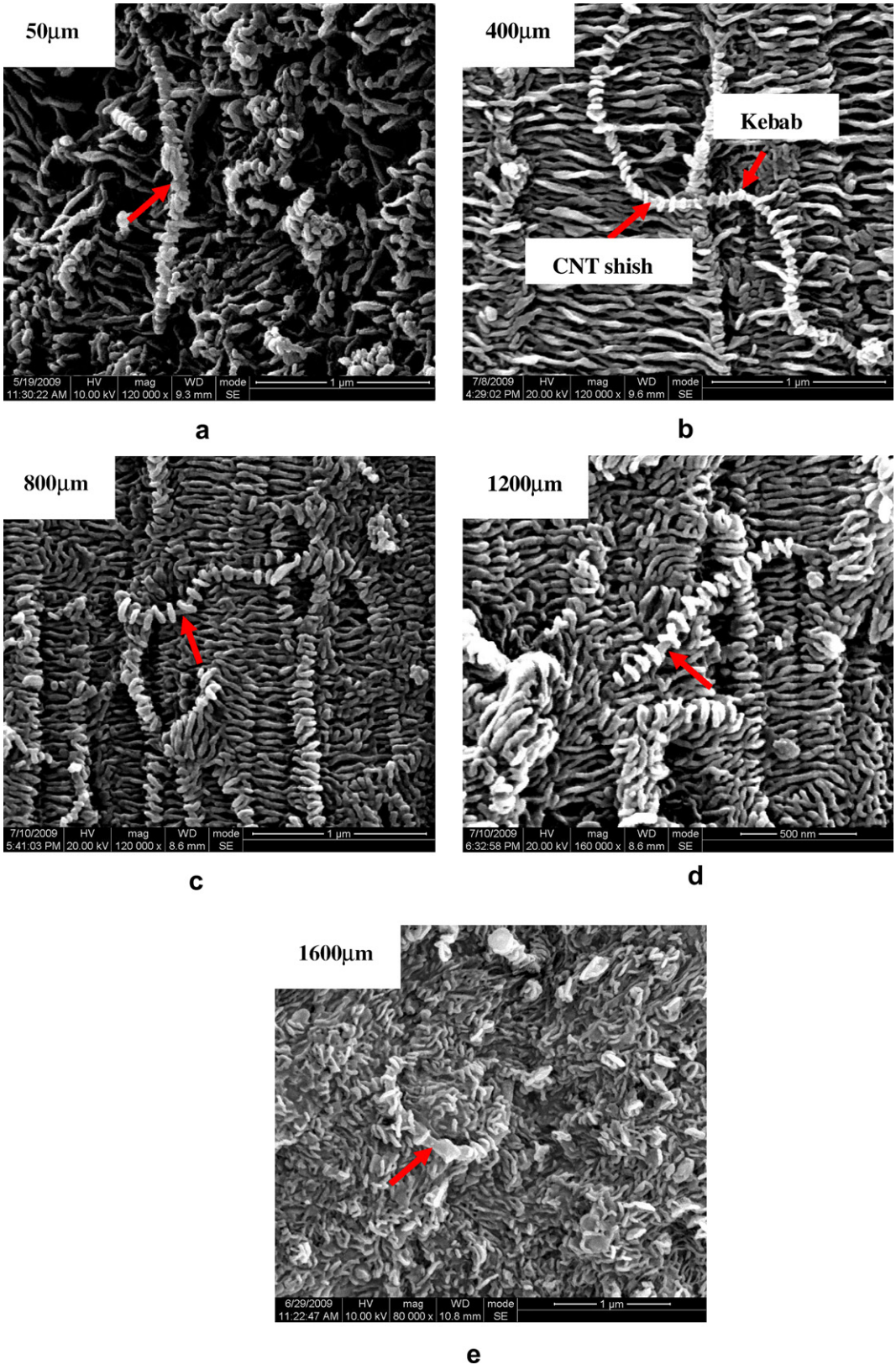

Fig. 6. SEM microphotographs of various layers of etched dynamic HDPE/CNTs composites along the thickness direction: (a) 50 μm; (b) 400 μm; (c) 800 μm; (d) 1200 μm; (e) 1600 μm.

layer (50 μm) and orientated layer (400 μm), as shown Fig. 8(a). The higher temperature peak at skin layer (50 μm) is ascribed to the re-crystallization melting of incomplete crystal; whereas, the higher one at 136 °C, increment for about 5 °C in the orientated layer (400 μm) can be considered as the melting of extended-chain crystalline structure (shish). It is well-documented that for

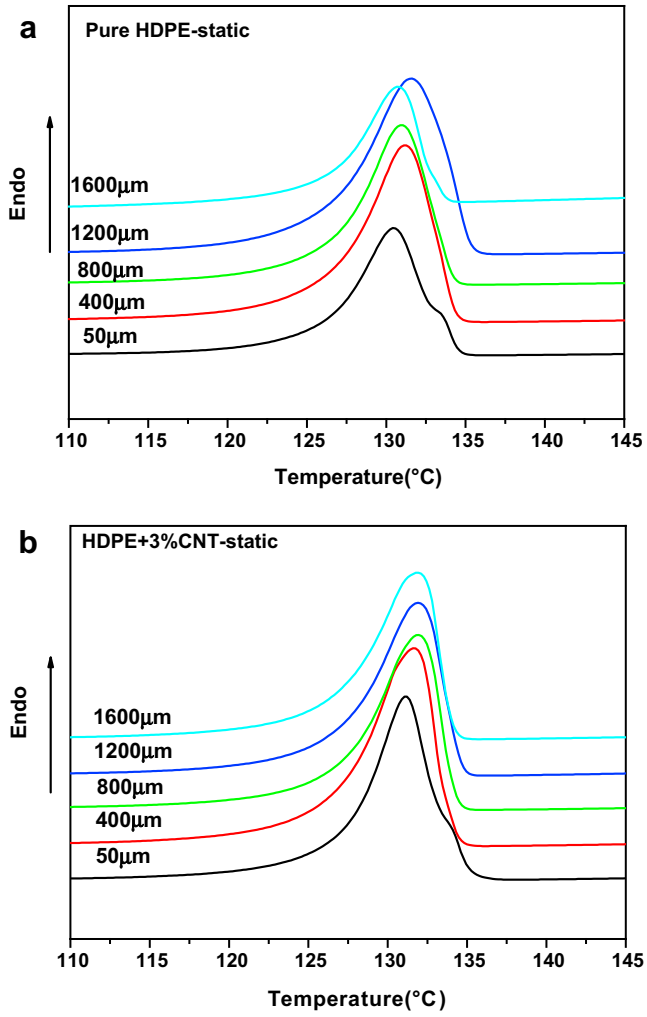

Fig. 7. DSC heating curves of various layers of static samples for (a) pure HDPE and (b) HDPE/MWCNTs composites.

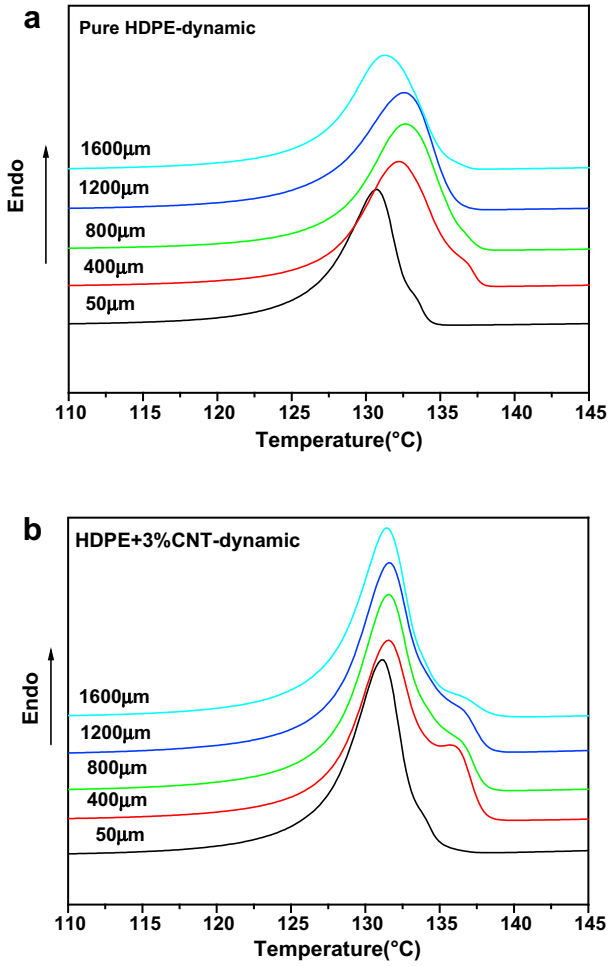

Fig. 8. DSC heating curves of various layers of dynamic samples for (a) pure HDPE and (b) HDPE/MWCNTs composites.

conventional shish–kebab structure, the longest chains play the key role for shish formation according to the coil–stretch theory proposed by Keller's [11–13], considering that only chains longer than a threshold chain length M^* undergo the coil–stretch transition under specified flow conditions. Obviously, seen from the DSC curves, because of the relative low molecular weight (M_w) of 1.2×10^5 of HDPE used, very few shish–kebab structure could be obtained, due to easy relaxation of short polymer chain. The easy relaxation can be further proved by that: in the core zone only one peak exists at 131 °C, which is lower than that in the oriented region.

The interesting finding is that with addition of MWCNTs, one can clearly observe two peaks in the heating curves from the skin zone to the core zone along the thickness direction. It is worthy to notice that the intensity of higher temperature peak is obviously stronger for the HDPE/MWCNTs composites than that of pure HDPE at 400 μm, indicating the promoted formation of extended-chain crystalline structure (shish) by adding MWCNTs. Besides, the intensity of higher temperature peak is gradually weak with the increasing depth of samples along the thickness. The ratio of higher temperature peak area to the first peak area shows a gradually decrease with increasing the depth of samples. And in the core of 1600 μm, the intensity of shish peak is obviously weak. The detailed data are listed in Table 2. It is clearly indicated that the temperature of second peak is higher than the first melting peak by 5 °C except for skin layer. Therefore, our results revealed that the incorporation of MWCNTs helps the formation of extended PE chains which may attach on the surface of MWCNTs. The origin of extended-chain shish must be very different between in dynamic pure HDPE and in dynamic composite. Two factors approve this statement. First, for the pure HDPE, the stretched chain shish appears only at an appropriate depth of 400 μm, whereas the PE shish exists within a wide region (400–1600 μm) in the composite. It can be logically deduced that the appearance of extended shish in a depth larger than 400 μm should be facilitated by adding of MWCNTs. Another evidence is that the percentage of shish fraction is very low in the pure HDPE, only for 5% at the depth of 400 μm, otherwise the PE shish fraction is high as a level of 20% in the oriented region of

Table 2
DSC analysis for melting peaks of HDPE/MWCNTs dynamic samples at various layers along the thickness directions.

	50 μm		400 μm		800 μm		1200 μm		1600 μm	
Peak center (°C)	130.9	134.0	131.5	136.8	131.7	136.1	131.5	136.1	131.3	136.1
Peak area	53.7	3.7	62.4	23.6	67.3	17.1	68.6	14.7	67.4	6.4
Ratio%	6.6		27.4		20.3		17.6		8.7	

dynamic composite, seeing the data presented in Table 2. Above all, DSC measurement supplies a strong support for our assumption that the hierarchy structure of NHSK strongly depends on the nucleation paths of MWCNTs. In shear layer, the shear stress induce the coil chain to be stretched, and stretched chains more easily wrap on the MWCNTs surface to form a PE shish layer, resulting in extended-chains (PE shish) melting at higher temperature. Due to the high nucleating capability of extended-chain shish, the MWCNTs wrapped with shish layer could attract more PE lamellae to periodically attach on them, obeying the "soft epitaxy" mechanism.

4. Conclusion

The orientation and crystalline morphology of HDPE/MWCNTs composites are investigated in detail by examining the lamellae and nanohybrid shish–kebab structure in the samples obtained via DPIM, layer by layer, along the sample thickness. A hierarchical structure with changed orientation and crystal structure along the thickness direction of molded bar is detected. Especially, for nanohybrid shish–kebab structure, at the skin layer and the core layer, the lamellae are randomly distributed on the surface of MWCNTs. While in the oriented layer, a typical nanohybrid shish–kebab structure that disk-shaped lamellae are periodically decorated along the MWCNTs axis is developed. Combining the results of SEM and DSC, it is reasonably believed that the formation of hierarchical structure of NHSK is mainly contributed to different nucleation paths of MWCNTs and chain relaxation of PE in the different depths along the sample thickness.

Acknowledgement

We would like to express our sincere thanks to the National Natural Science Foundation of China for Financial Support (50533050, 20874064, 50873063). And thanks also go to Dr. Liangbin Li and Prof. Guoqiang Pan of National Synchrotron Radiation Laboratory (NSRL) in University of Science and Technology of China for their help in synchrotron WAXD experiments.

References

[1] Thess A, Lee R, Nikolaev P, Dai HJ, Petit P, Robert J, et al. Science 1996;273:483.
[2] Tans SJ, Devoret MH, Dai HJ, Thess A, Smalley RE, Geerligs LJ, et al. Nature 1997;386:474.
[3] Walters DA, Ericson LM, Casavant MJ, Liu J, Colbert DT, Smith KA, et al. Appl Phys Lett 1999;74:3803.
[4] Hwang GL, Shieh YT, Hwang KC. Adv Funct Mater 2004;14:487.
[5] Banerjee S, Hemraj-Benny T, Wong SS. Adv Mater 2005;17:17–29.
[6] Grady BP, Pompeo F, Shambaugh RL, Resasco DE. J Phys Chem B 2002;106:5852.
[7] Zhao P, Wang K, Yang H, Zhang Q, Fu Q. Polymer 2007;48:5688.
[8] Lu KB, Grossiord N, Koning CE, Miltner HE, Mele BV, Loos J. Macromolecules 2008;41:8081.
[9] Chen QY, Bin YZ, Matsuo M. Macromolecules 2006;39:6528.
[10] Pennings AJ, Keil AM, Kolloid ZZ. Polymer 1965;205:160.
[11] Pope DP, Keller A. Colloid Polym Sci 1978;256:751.
[12] Miles MJ, Keller A. Polymer 1980;21:1295.
[13] Keller A, Odell JA. Nature 1984;312:98.
[14] Somani RH, Hsiao BS, Nogales A. Macromolecules 2001;34:5902.
[15] Liang S, Wang K, Chen DQ, Zhang Q, Du RN. Polymer 2008;49:4925.
[16] Li CY, Li LY, Cai WW, Kodjie SL, Tenneti KK. Adv Mater 2005;17:1198.
[17] Li LY, Li CY, Ni CY. J Am Chem Soc 2006;128:1692.
[18] Yue J, Xu Q, Zhang Z, Chen Z. Macromolecules 2007;40:8821.
[19] Zhang Z, Xu Q, Chen Z, Yue J. Macromolecules 2008;41:2868.
[20] Zhang F, Zhang H, Zhang Z, Chen Z, Xu Q. Macromolecules 2008;41:4519.
[21] Ning NY, Luo F, Pan BF, Zhang Q, Wang K, Fu Q. Macromolecules 2007;40:8533.
[22] Yang JH, Wang CY, Wang K, Zhang Q, Chen F, Du RN, et al. Macromolecules 2009;42:7016.
[23] Guan Q, Shen KZ, Li J, Zhu J. J Appl Polym Sci 1996;55:1797.
[24] Na B, Fu Q. Polymer 2001;43:7367.
[25] Cao W, Wang K, Zhang Q, Du RN, Fu Q. Polymer 2006;47:6857.
[26] Ning NY, Luo F, Wang K, Zhang Q, Chen F, Du RN, et al. J Phys Chem B 2008;112:14140.
[27] Wang Y, Zhang Q, Fu Q. Macromol Rapid Commun 2003;24:231.
[28] Wang Y, Zhang Q, Na B, Du R, Fu Q, Shen K. Polymer 2003;44:4261.